In vitro modeling for the aging of nanoplastics: physicochemical characteristics and effect on the biofilm formation of *Staphylococcus aureus*

Hasan Saygin
İstanbul Aydın Üniversitesi: Istanbul Aydin Universitesi
Aslı Baysal (aslibaysal@aydin.edu.tr)
Istanbul Aydin University https://orcid.org/0000-0002-0178-7808

Research Article

Keywords: nanoplastics, biofilm, secondary plastics, bacteria, human

Posted Date: August 27th, 2021

DOI: https://doi.org/10.21203/rs.3.rs-719241/v1

Abstract

Over the last decade, it has become clear that the pollution by plastic debris presents global societal, environmental, and human health challenges. Increasing scientific attention on the occurrence and influence of plastic particles, and their potential toxic effects on the environment are evident. However, humans are also exposed to plastics in daily life and very limited information is available concerning human health, especially aging process in biological fluids and the colonization of the bacteria on plastics due to transport the pathogens, causing the infectious is another vital problem. Moreover, various studies also observed the importance of the nano-sized particles since a lower size can increase the activity, surface area etc. Therefore, the aim of this study is to investigate the *in vitro* (artificial saliva, artificial lysosomal fluid, phagolysosomal simulant fluid, Gamble's solution) aging of plastic particles and the effect on the formation of *Staphylococcus aureus* biofilms with nanoplastics under *in vitro* conditions. We found that the surface properties of the nano-sized plastic particles changed according to the surrounding environment and surface deformation and the surface affinity to the biological activity was triggered with *in vitro* conditions due to higher hydroxyl index and carbon to nitrogen ratio. The results also showed that the *Staphylococcus aureus* biofilms formed with nanoplastics with the aging *in vitro* conditions. However, their levels and characteristic of extracellular polymeric substances were varied in these conditions with aging compared to control, and more basophilic extracellular polymeric substances were formed with these conditions.

1. Introduction

Nowadays, plastics are an emerging global problem because they are considered to be the most widely used industrial products, and they are routinely released into the environment in either direct or indirect ways (Saygin and Baysal 2020a). These plastic particles (or items/debris) are synthetic organic polymer particles and depending on their size, shape, or color, they can be classified as micro- (5 mm to 1 μm), submicron- (1 μm to 100 nm), and nano- (< 100 nm) plastics (Bradney et al. 2019; Baysal et al. 2020; Allan et al. 2021). Moreover, these plastic particles are grouped as primary and secondary plastic particles. Primary plastics can be either manufactured to have a certain size and purpose, and secondary plastics are fragmented from larger plastics (Ustabasi and Baysal 2020). This fragmentation can occur through physical and chemical processes in their surrounding environments from plastic packaging, plastic bags, or bottles, etc. Consequently, humans interact with these plastic particles. However, human exposure to plastic particles is largely uninvestigated and the studies have mostly focused on environmental living systems rather than human health (Bradney et al. 2019; Lu et al. 2019). Furthermore, the studies reported that plastic water bottles included varied concentrations (0.4–11.4 μg/L) and sizes (< 5μm) of plastic particles, and this can be one of the main sources for human exposure (Schymanski et al. 2018; Oßmann et al. 2018; Welle and Franz 2018; Koelmans et al. 2019; Cox et al. 2019). Concerning the potential sources for the contamination of bottled water with plastic particles, they are already suspected in the packaging (e. g. bottle and/or cap). Stress, fracture, or detached poly/oligomer groups of these parts of packages can cause fragmented plastic particles in bottled waters. Despite the increased

number of studies regarding the effect of such an environmental issue on human health, there have been some critical problems in these research papers; for instance, many of the studies have used pure/starting polymer material. However, plastic end-products include other additives (e.g., stabilizers, pigments) that significantly influence their behavior (sorption, degradation, etc.) (Allan et al. 2021; Ateia et al. 2020; Saygin and Baysal 2020a-d). As a result, end-product plastics rather than pure material are more representative to understand their actions on human health.

Moreover, the decrease in their size from micron to nano, that may also affect the surface area, reactivity, sorption, bioavailability, and biological impact on living systems (Ferreira et al. 2019; Yong et al. 2020; Saygin and Baysal 2020b,c). Additionally, human exposure can be unavoidably increased by the decreasing size of plastic particles. The behavior of microplastics has been widely documented for environmental systems such as marine invertebrates and fish. Although increasing efforts are focusing on the impacts of microplastics, the knowledge of the influence of nano-sized plastics is still scarce. More recently, the possible impacts of micro-and nanoplastics on mammalian cells and metabolism has begun to be investigated (Hwang et al. 2019; Lu et al. 2019). However, current knowledge is insufficient in terms of human exposure and its impact on human health (Yong et al. 2020).

The reactivity, bioavailability, and biological impact of plastic particles on living systems are altered by durability, dose, and exposure medium (Stefaniak 2010; Stebounova et al. 2011). Furthermore, the characterization of the physicochemical properties of nanoparticles under different conditions is essential for understanding their behavior and the potential effect on human health. To mimic the human-related conditions or cellular environment, *in vitro* modeling is often more desirable as a simple, reproducible, rapid, and cost-effective approach and various cellular fluids can be used (Stefaniak et al. 2005; Stefaniak 2010; Hu et al. 2013; Kastury et al. 2018). For example, artificial lysosomal fluid (ALF) simulates the intracellular environment and inflammatory conditions, phagolysosomal simulant fluid (PSF) mimics the chemical composition of lung alveolar macrophage, and a Gambles' solution (GS) represents the interstitial fluid deep within the lungs. However, there is no study considering the investigation of the plastic particles on human health using *in vitro* modeling that mimics the human-related conditions. There needs to be studies that integrate plastic particle characterization in a different medium, which includes the physicochemical characterization of surface properties.

Increasing plastic pollution can trigger the microbial contamination, such as biofilms, which become an important issue (Saygin and Baysal 2020d). Biofilms can be both a cause and cure for a range of global societal, environmental, and human health problems including the transfer of pathogens or toxic or non-toxic substances, antimicrobial tolerance and sanitation. Furthermore, the extracellular polymeric substances (EPS) of biofilms have a key role in the function or behavior of microbial biofilms (Sevior et al. 2019; Saygin and Baysal 2020b,d). In addition to that, increasing attention has been focused on understanding *Staphylococcus aureus* (*S. aureus*) biofilms' relationship to human disease due to their complex genetic nature, environmental relevance, and antibiotic resistance. Previous studies have shown that there is a strong connection between *S. aureus* occurrence and an increased risk of infections (e. g.,

skin infections and abscesses, pneumonia, meningitis, endocarditis, or toxic shock syndrome) (Archer et al. 2011; Kwiecinski et al. 2019).

Therefore, this study is the first aimed at investigating a more realistic proxy for the interaction processes of plastic particles under *in vitro* conditions. For this purpose, the most susceptible plastic particles that humans contact were aged in four different *in vitro* conditions (ALF, PSF, GS and saliva) from 2 h to 80 h, and the main surface characteristics were evaluated. Furthermore, the biofilm formation of the *S. aureus* in the presence of the plastic particles was examined under these *in vitro* conditions.

2. Materials And Methods

2.1 Reagents

The *S. aureus* (ATCC 25923) bacterial strains were obtained from American Type Culture Collection (ATCC). Tryptic soy broth (TSB), and other chemicals were acquired from Merck (Darmstadt, Germany). Ultrapure water was obtained using a Milli-Q water purification system (Merck, Darmstadt, Germany, conductivity 0.055 µS/cm at 25°C, pH 6.9).

2.2 Preparation of plastic particles and exposure to *in vitro* conditions

Commercially available plastic drinking water bottles were used to obtain plastic particles. The preparation of the plastic particles was based on our previous studies (Saygin and Baysal 2020a-d). Firstly, the bottles were washed with ultrapure water, allowed to dry on a clean bench, and milled with a stainless-steel render. The characterization procedures of the plastic particles explained in the next section and the particle size distribution and surface chemistry of the tested plastic particles were identified by Dynamic light scattering (DLS), Fourier-transform infrared spectrometry (FTIR), and Scanning electron microscopy with energy-dispersive X-ray spectroscopy (SEM/EDX) (Supplementary Fig. 1). The results showed that the tested plastic particles were < 100 nm and included carbon (C), oxygen (O), nitrogen (N), sodium (Na), and chloride (Cl). The FTIR spectrum of the particles showed that the bands, which were noticed at 1710 (C = O stretch), 1240 (C-O stretch), 1094 (C-O stretch), and 720 cm^{-1} (aromatic C-H out-of-plane bend) can be assigned the polyethylene terephthalate (PET), which is the most widely used polymer in plastic drinking water bottles.

To mimic the human-related conditions, *in vitro* modeling was applied through four different artificial human solutions (saliva, ALF, PSF, and GS). The artificial human solutions (saliva, ALF, PSF, and GS) and their chemical composition are shown in Supplementary Table 1. The fixed concentration of the plastic particles (50 mg) was mixed with each of the artificial human solutions (1000 mL) during 2h, 20h, 40h, 80h. Then, the plastic particles were removed from the suspensions by centrifugation, and then washed and dried. Three separate experimental set-ups were conducted for each incubation.

2.3 Characterization of plastic particles

The particle size distribution, surface chemistry and elemental composition of the plastic particles were characterized by DLS, FTIR, and SEM/EDX. Zetasizer Nano ZS (at 25°C, a 173° scattering angle, 4 mW He–Ne laser; Malvern Instruments, UK) were used for the DLS measurements. All the samples were analyzed in triplicates. The FTIR characterization of the plastic particles was carried out using a Bruker VERTEX 70 ATR instrument. The bulk was analyzed within the 4000–400 cm^{-1} range. All the samples were analyzed in triplicates and each spectrum was the sum of 64 scans. The EDX spectra were collected using an SEM/EDX spectrometer (QUANTA FEG 250, FEI, Thermo Fisher Scientific, Oregon, USA). All the samples were analyzed in triplicates.

The influence of *in vitro* conditions and incubation duration on the surface oxidation state was determined from the FTIR spectra by calculating the C-O (CI) and OH (HI) indices based on the relationships:

CI=(I1715 cm^{-1}/ I2966-64 cm^{-1}) and HI=(I3425 cm^{-1}/ I2966-64 cm^{-1}) respectively,

Where I1715 cm^{-1}: the intensity of C-O; I3425-23 cm^{-1}: the intensity of -OH; and I2966-64 cm^{-1}: the intensity of the methylene group (as control group).

The ratio of elemental oxygen to carbon (O/C) and carbon to nitrogen (C/N) was calculated from the EDX spectra.

2.4 Biofilm formation of *S. aureus* under *in vitro* conditions

To investigate the impact of the human-related conditions on the *S. aureus* biofilm formation with the plastic particles, *S. aureus* cells were incubated with the plastic particles and measured by using the crystal violet (CV) method according to our previous studies (Saygin and Baysal 2020a,d). For this purpose, plastic particles at the trace level (50 mg/L) which reflect human consumption and occurrences in drinking water bottles were examined for the culture-dependent biofilm formation (Hwang et al. 2019). Trace level were used due to being a more realistic proxy in the body and lung. The plastic particles were added onto the TSB prepared within which isolated bacteria were suspended. The bacteria exposed to the plastic particles were subjected to four different *in vitro* conditions: (i) one was a broth that was prepared with artificial saliva, (ii) the second broth was prepared using the ALF, (iii) the third broth was prepared with PSF, (iv) the fourth broth was prepared with GS. All four media were autoclaved for 15 min at 121°C before they were used in the tests. The controls for the procedure of the biofilm formation contained isolated bacteria, which were suspended in TSB broth prepared in ultrapure water. After 2 h, 20 h, 40 h, 80 h of incubation in a dark oven at 37°C, the plastics were removed from the growth media, placed in a glass Petri dish, and washed with ultrapure water. The plastics were air-dried at room temperature for 45 min in glass Petri dishes before staining with CV (1%) for an additional 45 min. The stained plastics were washed with ultrapure water, air-dried, and placed into a tube (2 mL), and ethanol (1 mL) was added for de-staining the plastics. Afterwards, the ethanol-containing solutions were pipetted to a well-plate, and the 595 nm of optical density (OD) was measured. The control for each sample involved the whole procedure and all the chemicals, but without any stained bacteria. The extent of the biofilm formation was

determined by the following formula: BF = OD–OD_C, where BF is the biofilm formation, OD is the OD at 595 nm of the stained bacteria and OD_C is the OD at 595 nm of the stained control samples containing only the bacteria-free medium (Saygin and Baysal 2020d).

To characterize the biofilms, the acidophilic and basophilic properties of the biofilms were investigated through the protein and carbohydrate content of the EPS. For this purpose, the EPS on the plastic particles was extracted at the end of the biofilm formation process (Saygin and Baysal 2020b,d). The plastic was collected, washed with de-ionized water, and dispersed into a suspension. The cell suspension was then immediately sonicated for 20 min at 4°C. The carbohydrate and protein content was determined in the EPS extracts (Saygin and Baysal 2020b,d). The carbohydrate content in the EPSs was determined by the phenol sulphuric acid method measured at 480 nm (Dubois et al. 1956). The protein content in the EPSs was determined by using the Bradford method (1976) at 595 nm by a microtiter UV–VIS spectrophotometer (Thermo Scientific MULTISKAN GO, Finland).

Biofilm formation of plastics and controls were prepared in five replicates at different times, and the results are reported as the averages of those replicates. The differences between control and samples, as well as the differences among samples, were analyzed by ANOVA with post hoc Tukey ($p < 0.05$). SPPS 17.0 software was applied for the significance and Spearman correlation (two-tailed) tests.

3. Results And Discussion

3.1 Impact of the *in vitro* aging on the surface characteristic of nanoplastics

The FTIR spectra of the nanoplastic particles incubated under *in vitro* conditions, which were saliva, ALF, PSF, and GS, is given in Fig. 1. The surface functional groups of the nanoplastic particles had different responses to the various cellular conditions of the artificial lung fluids (ALF, PSF and GS) and saliva. For instance, Fig. 1a shows the FTIR spectrum of the nanoplastic particles in the saliva. The spectrum indicated that it peaks at 3000 – 2800 cm^{-1} and 1550–1570 cm^{-1} appeared with the saliva incubation of the nanoplastic particles, and these peaks corresponded to the N-H stretching peaks. The N-related peaks can originate the saliva composition (as shown in Supplementary Table 1). The intensity of the double peaks of the C-O stretching between 1090–1250 cm^{-1} decreased with the incubation of the saliva. The decrease may be correlated to the balance of the available attaching sides on the nanoplastic particles. Additionally, the peaks of the N-related substances (1550–1570 cm^{-1}) and –OH bands (3200–3500 cm^{-1}) appeared with the incubation of the ALF on nanoplastic particles due to the –OH and N- related constituents in the fluid (Fig. 1b). The intensities of these peaks were increased with the incubation duration, which might be the association of the nanoplastic surfaces with the reaction of the N-, C- and O-related substances into the surrounding environment (Tavares et al. 2016). The C-O stretching peaks on nanoplastic particles at around 1290–1300 cm^{-1} were less intense at a longer incubation duration of ALF, which might relate to the available groups to attach. Contrarily to ALF, the N-related substances did

not attach to the surface of the nanoplastic particles with the PSF due to no N-related compounds in the PSF (Fig. 1c). This result may also indicate that nano-sized PET surfaces have an affinity to the N-related substances. Moreover, -OH bands appeared on the nanoplastic particles, but the highest intensity was obtained at a lower incubation duration with the PSF. The FTIR results also showed that it peaks at around 900–1800 cm^{-1}, which correlate with the C-H and C-O peaks were more intense with the PSF when compared to the ALF and the control. As shown in Fig. 1d, the -OH related bands between 3100–3700 cm^{-1} and the methylene group and vibrations of the ester C-O bond at around 1050–1100 cm^{-1} were significantly formed with the GS when compared to the control. Although the –OH groups decreased with the incubation of the GS, the doublet peak of the methylene group, and the vibrations of the ester C-O bond increased with the incubation of GS. All these spectrums indicated that the available functional groups and their intensities were changed according to the human related medium and duration of the incubation. These results also showed that the PET surface can be influenced by the surrounding environment. Despite some previous studies suggesting the impact of the surrounding environment on the plastic particles, none of these studies have investigated the influence of the human related conditions on the particle surface. The surface changing with the surrounding environment is also parallel with the study by Ioakeimidis et al. (2016). They examined the deformation potential of PET bottles into environmentally relevant conditions using FTIR, and they indicated that the deformation process of the PET surface seems to happen concurrently in the marine environment. Moreover, the shifts of –OH group, C-O, and N-H with the incubation time indicated the particles interacted with the surrounding medium. The –OH, N-H, and C-O band shifting, and formation of the free C-O groups indicate the coordination of the particle surface and medium (Yadav and Sontakke 2013; Givens et al. 2017; Tavares et al. 2016). Similar with these studies, the formation of C-O and N-H peaks also showed that the interaction occurred between plastic particles and human related medium.

In Fig. 2, the evolution of the -OH content and C-O content of the nanoplastic particles under *in vitro* conditions is presented for mimicking the possible surface deformation into human-related conditions (Rouillon et al. 2016; Liu et al. 2019; Saygin and Baysal 2020b,c). It can be stated that both the CI and HI of the nanoplastic particles were affected after incubation with saliva, ALF, PSF and GS. Based on the CI, the rate of the deformation for the different cellular conditions decreased at the lower incubation time (Fig. 2a) and these results indicated a protective effect on the chemical integrity of the plastic surface as assessed by FTIR, with a reduced CI (Awad et al. 2018). On the other hand, the CI index increased with the longer incubation time (80 h) in the saliva and PSF when compared to early exposures (2–40 h), and the CI values of the nanoplastic particles into the GS was not significantly influenced by the incubation duration. Additionally, the CI values of the nanoplastic particles in the ALF were responded differently when compared to the saliva, and the PSF and CI levels decreased with the increasing incubation. In the meantime, the lowest CI levels were obtained with the ALF condition with the longer incubation, which mimic the inflammatory (harsh) conditions of the lung. This result indicated that longer inflammatory conditions of the lung might protect the C-O backbones of the nanoplastic particles. The exposure to saliva and PSF had a similar reaction on the C-O backbones of the nanoplastic particles. This result

might be indicating that the C-O backbones of the nanoplastic particles cannot change after the ingestion of plastics through the mouth to the lung alveolar macrophage.

In contrast to the CI levels, the HI levels increased under *in vitro* conditions (Fig. 2b). The higher HI indicates the surface deformation. The level order at 2 h, 20 h, 40 h and 80 h were control < saliva < ALF < GS < PSF, control < saliva < PSF < GS < ALF, control < PSF < GS < saliva < ALF, and PSF = GS < control < saliva < ALF. These results also indicated that early exposure could cause the highest oxidation of the nanoplastic particles under *in vitro* conditions. The highest oxidation at the earliest exposure was obtained in the alveolar macrophages conditions (PSF) as the PSF acts as a protector for the lung from inhaled substances (Oberdörster et al. 1992). This result suggested that the lung alveolar macrophages can degrade the -OH groups onto the plastics to protect the lung. However, over time, the oxidation levels (HI) of the nanoplastic particles reduced, and the results showed that the -OH backbone was degraded in the early exposure of the PSF and GS; then the -OH backbone was the protector, except for in the saliva and ALF (Awad et al. 2018). Moreover, the HI of the nanoplastic particles increased under the inflammatory conditions (ALF) with the incubation. This result suggested that the oxidation of the surface increased under inflammatory conditions (ALF) in time, while the C-O backbone was protected.

The aging in surrounding environment can also influence the elemental distribution of the nanoplastic particles and their surface affinity. To examine the effect of *in vitro* aging on the elemental distribution of the nanoplastic particles, the O/C, and C/N ratios were calculated using O, C, and the N content obtained by the EDX spectrum. These ratios are also an indicator of the surface deformation and affinity to the biological activity (Luo et al. 2020; Saygin and Baysal 2020b,c; Chen et al. 2015). As indicated in Fig. 3a, the O/C value of the nanoplastic particles was significantly higher after incubation with the ALF and GS. This finding can be explained by the attachment of the –OH groups on the surface and reduced carbonyl compounds. The higher O/C values indicated the surface deformation in the ALF and GS when compared to the control (Luo et al. 2020; Saygin and Baysal 2020b,c). However, the incubation duration did not significantly influence the O/C values of the nanoplastic particles in the ALF and GS due to the detachment of the –OH groups, the attachment of the methylene group, and the vibrations of the ester C-O bond on the surface. On the other hand, the O/C ratio of nanoplastic particles reduced into the PSF and saliva compared to control. The O/C ratio in these environments was also influenced by the incubation duration in these fluids. The O/C ratios of the nanoplastic particles in the saliva were lower at the early incubations when compared to the longer incubation and their controls, which increased. Contrarily, the O/C ratio at longer incubation was lower than early incubation into the PSF. This result indicated that the surface deformation can start with the increasing incubation in the saliva. However, the lower O/C values also indicated surface protectivity. These results can be correlated with the CI values. The higher O/C value obtained at the lower incubation when compared to increasing incubations for PSF. This result can be explained that the –OH attachment was the highest level at early exposure when compared to longer durations for the PSF and negatively correlated with CI. Furthermore, Fig. 3b shows the C/N ratios to indicate the nanoplastic surfaces' affinity to the biological activities with the *in vitro* aging. The results showed that the C/N values were lower in all the tested conditions. This result showed the surface can open the biological activities due to increased N content and formation N-related functional groups. On

the other hand, the C/N values demonstrated a time-dependent increase in the ALF and the saliva, and they were greater compared to GS and PSF. The higher time-dependent increase of C/N ratio in saliva correlated with CI levels, but it has negative relationship with HI levels. Contrarily to the saliva, the C/N ratio in ALF has negative correlation with CI and positive correlation with HI. The higher CI indicates the surface deformation, therefore, these results indicated that the surface deformation by carbonyl groups and protection of hydroxyl groups occurred in saliva, and this situation may limit the biological activity. However, increased surface biological affinity was obtained by the protection of carbonyl groups and deformation of hydroxyl groups on the plastics in ALF.

3.2 Biofilm formation of nanoplastic particles under *in vitro* conditions

The formation of the *S. aureus* biofilms and their EPS characteristics were evaluated in the presence of the nanoplastic particles with 2–80 h incubation under *in vitro* conditions (Fig. 4). The results showed that biofilm formation was varied according to the aging environment. For example, biofilms increased by the aging in the presence of nanoplastics in the controlled conditions. Moreover, the results obtained from saliva and ALF condition showed that the formation was not changed during the aging, except decrease at 2 h in saliva and 20 h in ALF aging. Unfortunately, this finding cannot be correlated with surface properties of nanoplastics. On the other hand, the biofilm formation showed similar responses in PSF and GS with nanoplastics. This result can be originated by the surface changes of nanoplastics with these environments. Similar behavior of biofilmformation can be explained that lower C/N values with time can support the biological affinity of nanoplastics in PSF and GS since the C/N levels positively correlated with O/C levels and CI levels. Furthermore, the order of the biofilm formation at 2 h, 20 h, 40 h, and 80 h were saliva < GS < PSF < control < ALF, ALF < PSF < GS < control < saliva, saliva < ALF < GS < control < PSF, and GS < PSF < saliva < ALF < control, respectively. The biofilm formation behavior in the saliva, ALF and GS mostly negatively influenced the CI values and positively affected the C/N values. However, the responses into the PSF were different. Moreover, the reduced biofilm formation with the incubation time can be explained by the increased C/N that indicated the decrease in the biological activity when compared to the control. Besides, the results showed that early exposure into the inflammatory conditions promoted the biofilm formation of the nanoplastics, and as time passed, the possibility of the biofilm formation was lower than the control due to the deformation of surface.

The biofilm characteristics were examined through the acidophilic and basophilic properties of the EPS (Fig. 4). For this purpose, the protein and carbohydrate ratio were calculated. The result showed that the acidophilic character of the biofilms into the saliva, ALF, PSF, and GS were greater than the control. These results indicated that the biofilms into *in vitro* conditions can have more affinity to the cationic substance compared to the control. Moreover, the basophilic characteristic of the biofilms into the ALF and GS reduced with the incubation time when compared to the control; this result can be explained by the surface properties of nanoplastics in these media. however, similarly with the control, the basophilic character of the biofilms in the saliva and PSF were promoted with the incubation time.

4. Conclusion

This study is the first to investigate the surface behaviors of nanoplastic particles with *in vitro* aging to mimic the human cellular environment. The results showed that surface nanoplastic particles changed under the *in vitro* conditions. The surface of the nanoplastic particles attached with N-related substance and –OH functional groups under intracellular lung environment and inflammatory conditions (ALF), and N-related and –OH groups on the surface increased with time. Moreover, the biofilms formed with the nanoplastic particles under these conditions. However, these biofilms also had more acidophilic characteristics when compared to the control. These results suggested that more cationic substances might be attached to these biofilms under a cellular environment and inflammatory conditions.

Based on the results, we hypothesize that the use of a bio-relevant environment provides realistic estimates of the surface characteristics of nanoplastic particles and their biofilm formation respecting the biological activities. The changes in the surface properties of nanoplastics and their biofilm response showed that human exposure to the nanoplastics needs further attention, especially in terms of the interactions of the plastic particles with biological substances in a different cellular environment. These findings are also important to understand the toxicity of plastics and their interaction with biological substances or other natural/antrophogenic substances. Moreover, the results from this study can be used for the desinging new bioavaliable materials.

Declarations

Ethics approval and consent to participate: Not applicable. The manuscript does not report on or involve the use of any animal or human data or tissue.

Consent for publication: Not applicable. The manuscript does not contain data from any individual person.

Availability of data and materials: The datasets used and/or analysed during the current study are available from the corresponding author on reasonable request.

Competing interests: The authors did not receive support from any organization for the submitted work.

Funding: The authors have no relevant financial or non-financial interests to disclose.

Authors' contributions: HS: Conceptualization, Investigation, Methodology, Formal analysis, Writing- Original draft preparation. AB: Investigation, Resources, Methodology, Writing- Original draft preparation.

References

Allan J, Belz S, Hoeveler A, Hugas M, Okuda H, Patri A, Rauscher H, Silva P, Slikker W, Sokull-Kluettgen B, Tong W, Elke A. (2021) Regulatory landscape of nanotechnology and nanoplastics from a global perspective. Regul Toxicol Pharmacol. 122:104885. https://doi.org/10.1016/j.yrtph.2021.104885

Archer NK, Mazaitis MJ, Costerton JW, Leid JG, Powers ME, Shirtliff ME. (2011) Staphylococcus aureus biofilms: properties, regulation, and roles in human disease. Virulence. 2(5):445-59. https://doi.org/10.4161/viru.2.5.17724

Ateia M, Zheng T, Calace S, Tharayil N, Pilla S, Karanfil S. (2020) Sorption behavior of real microplastics (MPs): insights for organic micropollutants adsorption on a large set of well-characterized MPs. Sci. Total Environ., 720:137634. https://doi.org/10.1016/j.scitotenv.2020.137634

Awad SA, Fellows CM, Mahini SS. (2018) Effects of accelerated weathering on the chemical, mechanical, thermal and morphological properties of an epoxy/multi-walled carbon nanotube composite. Polymer Testing 66:70–77. https://doi.org/10.1016/j.polymertesting.2017.12.015

Baysal A, Saygin H, Ustabasi GS. (2020) Microplastic occurrences in sediments collected from Marmara Sea-Istanbul, Turkey. Bull Environ Contam Toxicol. 105(4):522-529. https://doi.org/10.1007/s00128-020-02993-9

Bradford MM. (1976) A rapid and sensitive method for the quantitation of microgram quantities of protein utilizing the principle of protein-dye binding. Anal. Biochem. 72:248-254.

Bradney L, Wijesekara H, Palansooriya KN, Obadamudalige N, Bolan NS, Ok YS, Rinklebe J, Kim KH, Kirkham MB. (2019) Particulate plastics as a vector for toxic trace-element uptake by aquatic and terrestrial organisms and human health risk. Environ Int. 131:104937. https://doi.org/10.1016/j.envint.2019.104937.

Chen, W., Chen, M., and Zhou, X. (2015). Characterization of biochar obtained by co-pyrolysis of waste newspaper with high-density polyethylene. BioRes. 10(4):8253-8267.

Cox KD, Covernton GA, Davies HL, Dower JF, Juanes F, Dudas SE. (2019) Human consumption of microplastics. Environ Sci Technol. 53(12):7068-7074. Epub 2019 Jun 5. Erratum in: Environ Sci Technol. 2020 1;54(17):10974. https://doi.org/10.1021/acs.est.9b01517

Dubois M, Gilles KA, Hamilton JK, Rebers P, Smith F. (1956) Colorimetric method for determination of sugars and related substances. Anal. Chem. 28: 350-356.

Ferreira I, Venâncio C, Lopes I, Oliveira M. (2019) Nanoplastics and marine organisms: What has been studied? Environ Toxicol Pharmacol. 67:1-7. https://doi.org/10.1016/j.etap.2019.01.006

Hu JL, Nie SP, Min FF, Xie MY. (2013) Artificial simulated saliva, gastric and intestinal digestion of polysaccharide from the seeds of Plantago asiatica L. Carbohydr Polym. 92(2):1143-50. https://doi.org/10.1016/j.carbpol.2012.10.072

Hwang J, Choi D, Han S, Choi J, Hong J. (2019) An assessment of the toxicity of polypropylene microplastics in human derived cells. Sci Total Environ. 684:657-669. https://doi.org/10.1016/j.scitotenv.2019.05.071

Ioakeimidis, C., Fotopoulou, K., Karapanagioti, H. et al. (2016) The degradation potential of PET bottles in the marine environment: An ATR-FTIR based approach. Sci Rep. 6:23501. https://doi.org/10.1038/srep23501

Kastury F, Smith E, Karna RR, Scheckel KG, Juhasz AL. (2018) Methodological factors influencing inhalation bioaccessibility of metal(loid)s in PM2.5 using simulated lung fluid. Environ Pollut. 241:930-937. https://doi.org/10.1016/j.envpol.2018.05.094

Koelmans AA, Mohamed Nor NH, Hermsen E, Kooi M, Mintenig SM, De France J. (2019) Microplastics in freshwaters and drinking water: Critical review and assessment of data quality. Water Res. 15(155):410-422. https://doi.org/10.1016/j.watres.2019.02.054

Kwiecinski JM, Jacobsson G, Horswill AR, Josefsson E, Jin T. (2019) Biofilm formation by Staphylococcus aureus clinical isolates correlates with the infection type. Infect Dis (Lond). 51(6):446-451. https://doi.org/10.1080/23744235.2019.1593499

Lu L, Luo T, Zhao Y, Cai C, Fu Z, Jin Y. (2019) Interaction between microplastics and microorganism as well as gut microbiota: A consideration on environmental animal and human health. Sci Total Environ. 667:94-100. https://doi.org/10.1016/j.scitotenv.2019.02.380

Luo H, Li Y, Zhao Y, Xiang Y, He D, Pan X (2020) Effects of accelerated aging on characteristics, leaching, and toxicity of commercial lead chromate pigmented microplastics. Environ Pollut 257:113475. https://doi.org/10.1016/j.envpol.2019.113475

Oßmann BE, Sarau G, Holtmannspötter H, Pischetsrieder M, Christiansen SH, Dicke W. (2018) Small-sized microplastics and pigmented particles in bottled mineral water. Water Res. 141:307-316. https://doi.org/10.1016/j.watres.2018.05.027

Rouillon C, Bussiere PO, Desnoux E, Collin S, Vial C (2016) Is carbonyl index a quantitative probe to monitor polypropylene photodegradation? Polym Degrad Stab 128:200. https://doi.org/10.1016/j.polymdegradstab.2015.12.011

Saygin H, Baysal A. (2020a) Similarities and discrepancies between bio-based and conventional submicron-sized plastics: ın relation to clinically ımportant bacteria. Bull Environ Contam Toxicol. 105(1):26-35. https://doi.org/10.1007/s00128-020-02908-8

Saygin H, Baysal A. (2020b) Insights into the degradation behavior of submicroplastics by Klebsiella pneumoniae. J Polym Environ 29:958–966 (2021). https://doi.org/10.1007/s10924-020-01929-y.

Saygin H, Baysal A. (2020c) Degradation of subμ-sized bioplastics by clinically important bacteria under sediment and seawater conditions: Impact on the bacteria responses, J Environ Sci Heal A. 56(1):9-20. https://doi.org/10.1080/10934529.2020.1833591.

Saygin H, Baysal A. (2020d) Biofilm formation of clinically ımportant bacteria on bio-based and conventional micro/submicron-sized plastics. Bull Environ Contam Toxicol. 105(1):18-25. https://doi.org/10.1007/s00128-020-02876-z

Schymanski D, Goldbeck C, Humpf HU, Fürst P. (2018) Analysis of microplastics in water by micro-Raman spectroscopy: Release of plastic particles from different packaging into mineral water. Water Res. 129:154-162. https://doi.org/10.1016/j.watres.2017.11.011

Stebounova LV, Guio E, Grassian VH. (2011) Silver nanoparticles in simulated biological media: a study of aggregation, sedimentation, and dissolution. J Nanopart Res 13:233–244. https://doi.org/10.1007/s11051-010-0022-3

Stefaniak AB, Guilmette RA, Day GA, Hoover MD, Breysse PN, Scripsick RC. (2005) Characterization of phagolysosomal simulant fluid for study of beryllium aerosol particle dissolution. Toxicol In Vitro. 19(1):123-34. https://doi.org/10.1016/j.tiv.2004.08.001

Stefaniak AB. (2010) Persistence of tungsten oxide particle/fiber mixtures in artificial human lung fluids. Part Fibre Toxicol. 7(1):38. https://doi.org/10.1186/1743-8977-7-38

Tavares LB, Boas CV, Schleder GR, Nacas AM, Rosa DS, Santos DJ. (2016) Bio-based polyurethane prepared from Kraft lignin and modified castor oil. EXPRESS Polym Lett. 10(11):927–940. https://doi.org/10.3144/expresspolymlett.2016.86

Ustabasi GS, Baysal A. (2019) Occurrence and risk assessment of microplastics from various toothpastes. Environ Monit Assess. 191(7):438. https://doi.org/10.1007/s10661-019-7574-1

Welle F and Franz R. (2018) Microplastic in bottled natural mineral water - literature review and considerations on exposure and risk assessment. Food Addit Contam Part A Chem Anal Control Expo Risk Assess. 35(12):2482-2492. https://doi.org/10.1080/19440049.2018.1543957

Yong CQY, Valiyaveetill S, Tang BL. (2020) Toxicity of microplastics and nanoplastics in mammalian systems. Int J Environ Res Public Health. 17(5):1509. https://doi.org/10.3390/ijerph17051509

Figures

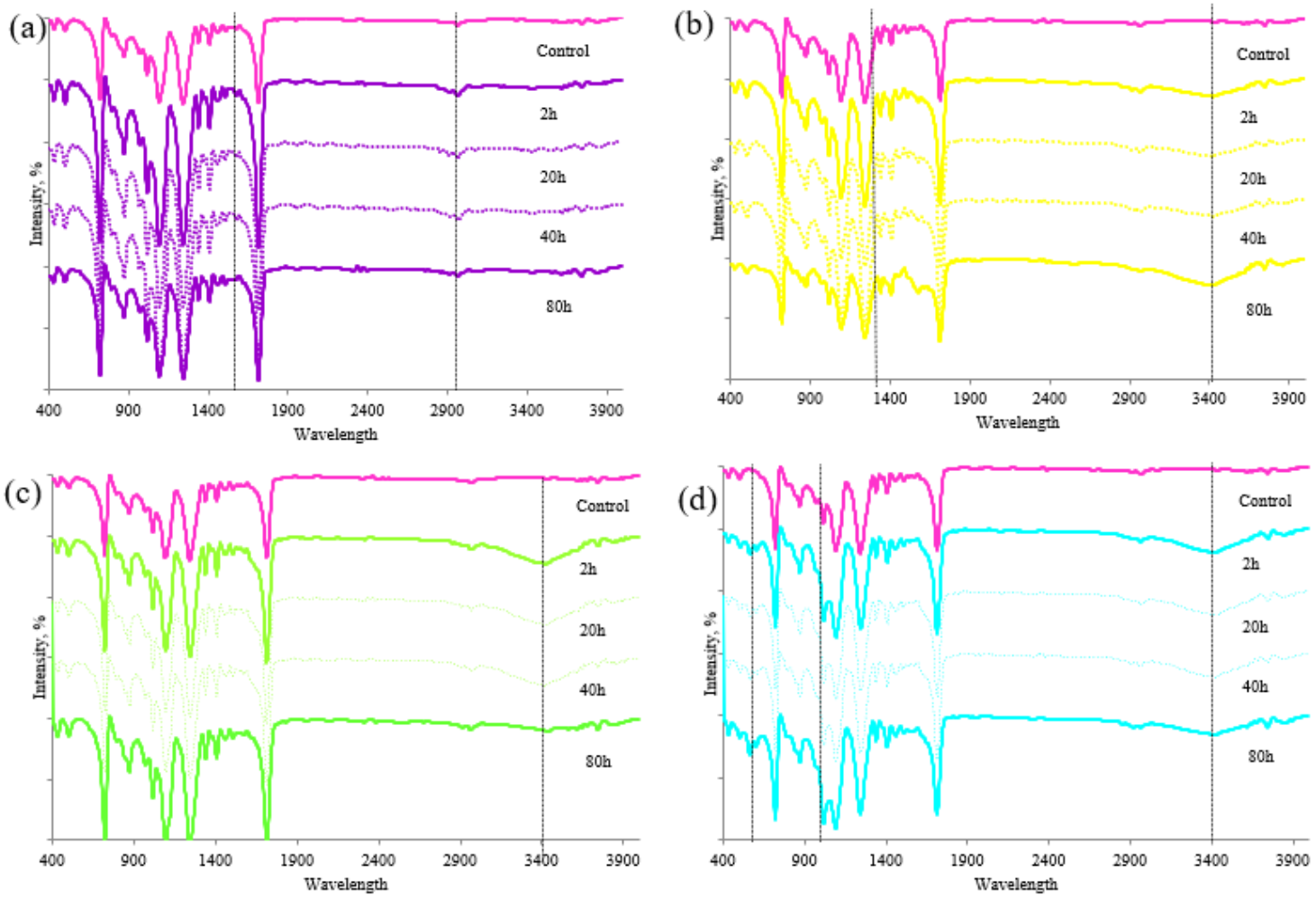

Figure 1

FTIR spectrum of aged nanoplastic particles under in vitro conditions at various incubation times.

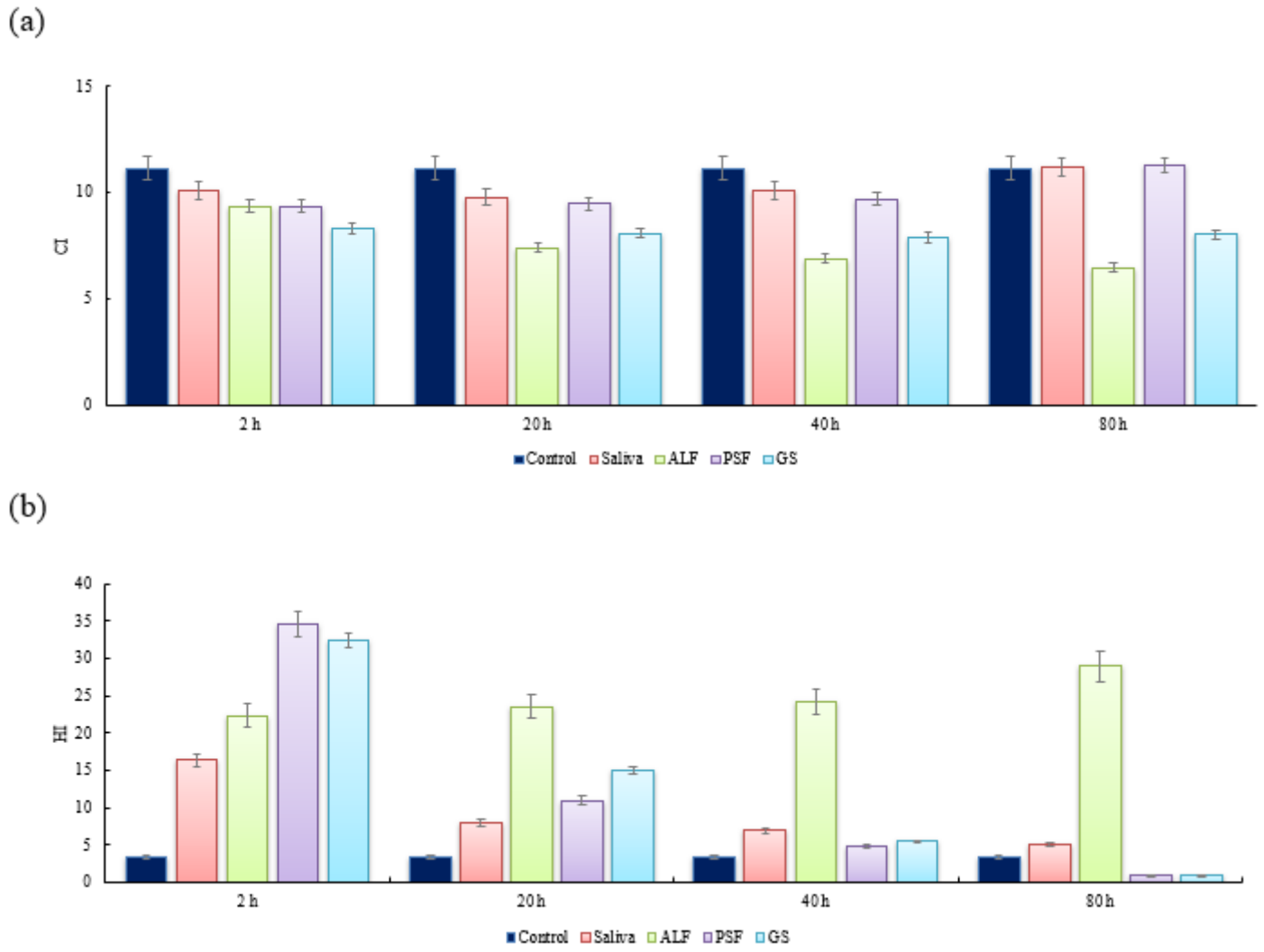

Figure 2

(a) CI (carbonyl index) and (b) HI (hydroxyl index) of nanoplastic particles with the in vitro aging. N=3

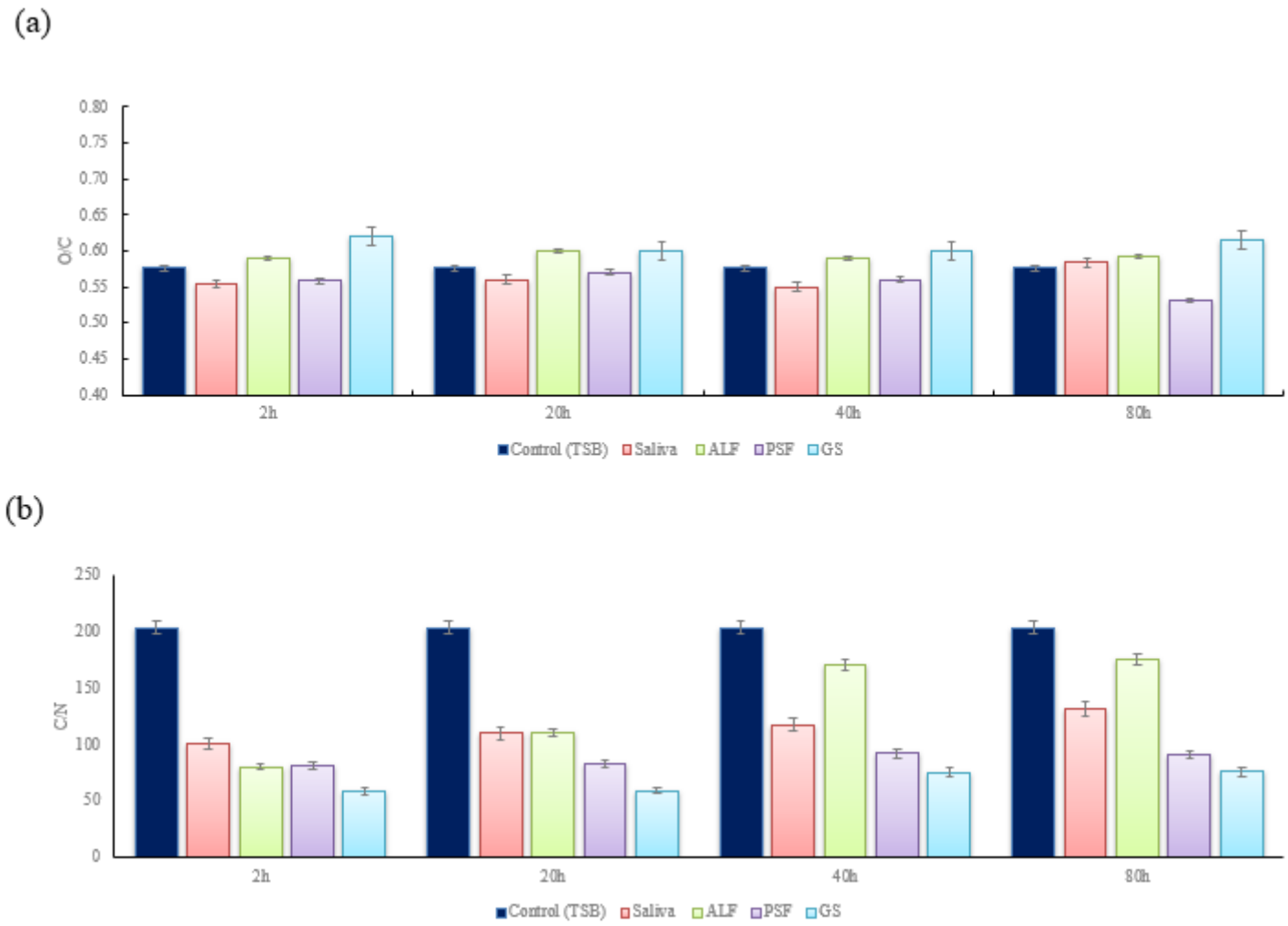

Figure 3

(a) O/C and (b) C/N ratio of nanoplastic particles with the in vitro aging. C, O and N contents obtained from EDX. N=3

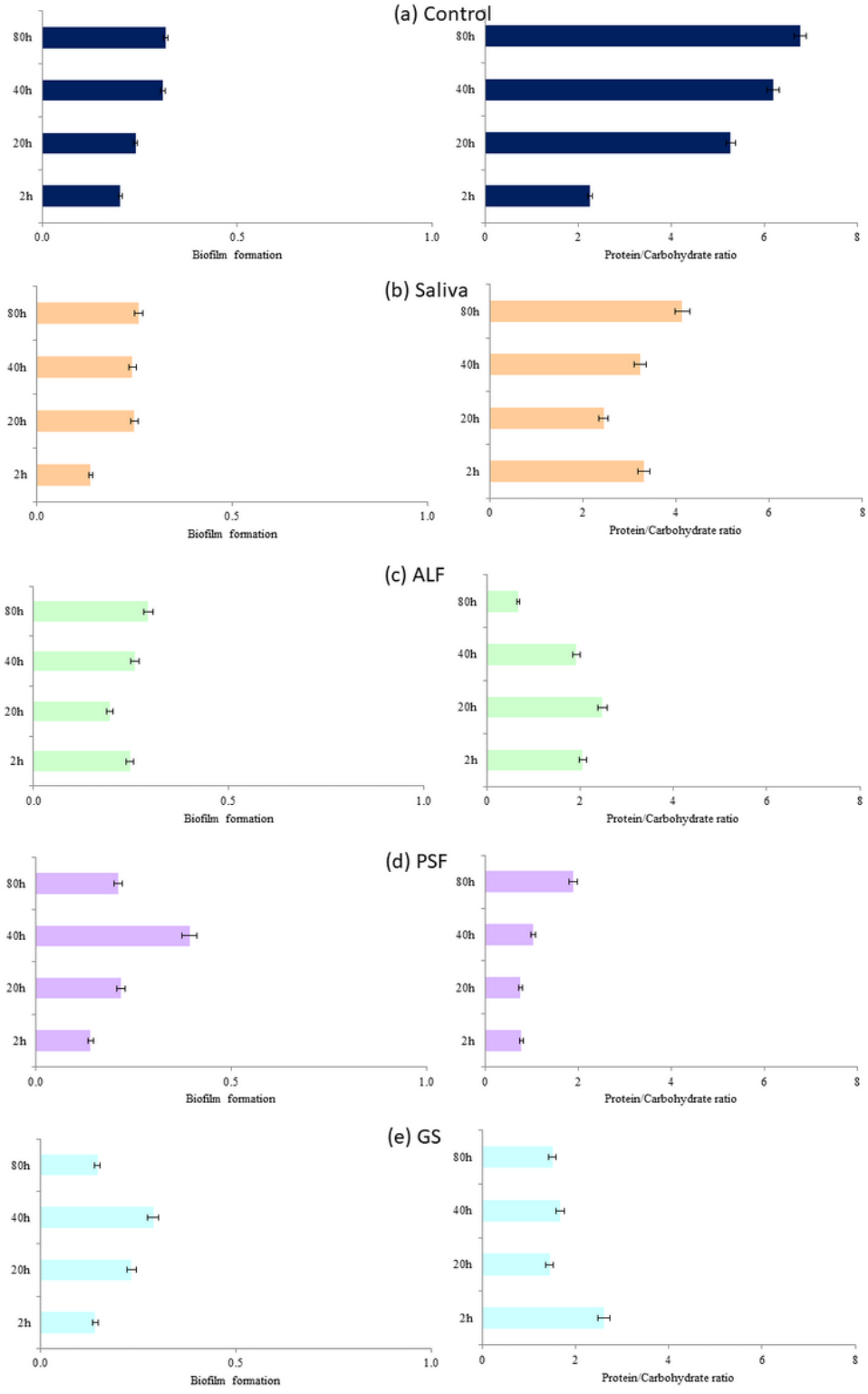

Figure 4

Biofilm formation of S. aureus and the EPS characteristics (protein to carbohydrate ratio) in the presence of nanoplastics under (a) Control, (b) Saliva, (c) ALF, (d) PSF, and (e) GS. N = 5

Supplementary Files

This is a list of supplementary files associated with this preprint. Click to download.

- supplementarymaterials.docx